Drug Development and Industrial Pharmacy, 35:12–18, 2009
Copyright © Informa UK, Ltd.
ISSN: 0363-9045 print / 1520-5762 online
DOI: 10.1080/03639040802130087

informa
healthcare

Collisional Solute Release from Thermally Activated Lipid Particles

Pengyun Zeng, Jeffrey Mahlberg, and Timothy Scott Wiedmann
Department of Pharmaceutics, University of Minnesota, Minneapolis, MN, USA

Solid lipid particles were evaluated for their potential as a thermo-activated drug delivery system. Submicron-sized diphenylhexatriene (DPH)/myristyl alcohol particles were produced by an atomization/drying process and the release rate of DPH into sodium dodecyl sulfate (SDS) micellar solutions was measured. The results showed that the presence of micelles and thermal activation was necessary and sufficient for the release of DPH. The initial rate of DPH release was linear for most systems. However, nonlinearity was noted at low micelle concentrations where the rate decreased with time due to the loss of sink conditions with the rising concentration of DPH in the micellar solution. Also at high micelle and particle concentrations, the rate increased with time, which may be due to a loss of particle integrity. Analyzing the data from a design study, the release rate was found to be linearly proportional to particle concentration. In contrast, the rate of release increased with micelle concentration in a nonlinear manner and appeared to approach a plateau at high micelle concentrations. The decrease in rate as the micelle concentration increased is suggestive of a saturable process and may involve a collision-based mechanism.

Keywords diphenylhexatriene; thermal release; collision theory; fluorescence; myristyl alcohol

INTRODUCTION

The potential of nanoparticles for drug delivery has led to a great interest in the use of solid lipid particles (LPs) (Mehnert & Mader, 2001; Wong, Bendayan, Rauth, Li, & Wu, 2007; Xiang et al., 2007). One attractive feature of solid LPs is that they can be formulated with components that have melting temperatures just above 37°C. With such a system, the rate of drug release can be dramatically increased when the particle is warmed. There are a number of safe means to cause both general as well as selective heating of particles (Lao & Ramanujan, 2004). Moreover, spatially selective heating can then provide for site specific and temporally controlled drug release, which would lead to a higher local concentration and lower systemic concentration (Aoki et al., 2004; Needham, Anyarambhatla, Kong, & Dewhirst, 2000).

The solid lipid nanoparticles are typically 100–1,000 nm in diameter and can be prepared by a number of different processes including hot and cold emulsion/homogenization, solvent diffusion, and spray drying (Mehnert & Mader, 2001). Because the particles are small and solid, the release rate is often characterized by a significant burst effect due to the large surface to volume ratio (Venkateswarlu & Manjunath, 2004; Wong et al., 2007). This is followed by a slower rate of release of drug. Aside from these papers, most have focused on pharmacological/therapeutic endpoints to evaluate the utility of this approach in delivering drugs (Wissing, Kayser, & Muller, 2004; Zara, Bargoni, Cavalli, et al., 2002; Zara, Cavalli, Bargoni, et al., 2002).

Of those that have examined the release of solutes in vitro, the rate was dependent on particle size and aqueous solubility of the drug (zur Muhlen, Schwarz, & Mehnert, 1998). In the case of hydrophobic compounds, the rate was also dependent on the surfactant concentration in the receptor media. Specifically, micelle solubilization was found to be an essential means for dissolution of the water insoluble compounds. For larger sized particles (>100 nm), significant resistance to the release of hydrophobic compounds is expected from the diffusional boundary layer (Chan, Evan, & Cussler, 1976). In contrast, the small size of the nanoparticles gives rise to relatively rapid diffusion and as such, they can not be considered being stationary. In this case, both the diffusion of the micelle as well as diffusion of the nanoparticle should be considered. Therefore, it may be better to conceptualize the release as a result of exchange of drug between the micelle and particle during a collision. This approach was used to examine release of fatty acids in bile salt micellar solutions (Chan et al., 1976).

Here, submicron-sized LPs were prepared, and the initial rates of release of the hydrophobic fluorescent compound, diphenylhexatriene, into sodium dodecyl sulfate (SDS) micellar solutions were determined as a function of the concentration of LPs and micelles. The presence of micelles and thermal activation was necessary and sufficient for the release of diphenylhexatriene (DPH), and the kinetics of the release involved a process that appeared to be saturable with micelle concentration.

Address correspondence to Timothy Scott Wiedmann, Department of Pharmaceutics, University of Minnesota, 308 Harvard St. SE, Minneapolis, MN 55455, USA. E-mail: wiedm001@tc.umn.edu

EXPERIMENTAL PROCEDURE

Materials

Myristyl alcohol (MA) was purchased from MP Biomedicals, LLC. (Solon, OH, USA) diphenylhexatriene was purchased from Aldrich Chemical Co. (Milwaukee, WI, USA) and SDS, monosodium and disodium hydrogen phosphate buffer, and sodium chloride were purchased from Sigma Chemical Co. (St. Louis, MO, USA).

Methods

LPs were prepared by an aerosolization/drying process as described earlier (Hitzman, Elmquist, Wattenberg, & Wiedmann, 2006; Wiedmann & Hitzman, 2004). Briefly, 196.5 mg MA and 2.9 mg DPH were dissolved in a mixture of 8.81 g ethanol and 7.67 g acetone that was atomized into droplets using a 1.7 MHz ultrasonic driver and a custom-built glass baffle with an air stream flowing at 0.5 L/min. The volatile solvent was removed from the droplets by a custom-built, stainless-steel reflux dryer, and the dried DPH/MA particles were collected on a microfiber filter with the introduction of additional air to produce a total air flow rate of 4 L/min.

Differential scanning calorimetry (DuPont 910, DuPont, Wilmington, DE, USA) was used to measure the phase transition temperature and heat of fusion of pure MA and the LPs. The scanning rate was 5°C/min. The melting point was calculated using the associated software in which the most rapidly rising portion of the endotherm was extrapolated to the baseline.

The particle size distribution in solution was determined by dynamic light scattering (Nicomp, Santa Barbara, CA, USA). The particles were dispersed into 0.01% SDS/phosphate buffer and size was determined. In addition, the size was determined by dispersing the particles into 10% SDS, incubating at 42°C for 90 min, and then diluting the dispersion to reduce the SDS concentration to 0.1%.

Fourier-transform pulsed-field gradient spin-echo (PFG-SE) ^{1}H NMR diffusion measurements of the SDS solutions were performed on nonspinning samples in thin-wall 5-mm tubes on a Varian 600 MHz spectrometer (Palo Alto, CA, USA). A stimulated spin echo pulse sequence was used, and the transformed intensity was analyzed by the following equation (Stilbs, 1982):

$$A(\tau_1+\tau_2)=\frac{1}{2}A(0)\exp\left(\frac{-2\tau_1}{T_2}\right)\exp\left[\frac{-(\tau_2-\tau_1)}{T_2}\right]\exp\left\{-(\gamma G\delta)^2 D\left(\frac{\Delta-\delta}{3}\right)\right\}$$

where $A(\tau_1 + \tau_2)$ is the peak intensity at time, $\tau_1 + \tau_2$, $A(0)$ is the peak intensity at time, 0, T_2 is the spin-spin relaxation time, T_1 is the spin-lattice relaxation time, γ is the gyromagnetic ratio, G is the strength of field gradient, δ is the duration of field gradient, D is the diffusion coefficient, and Δ is the time interval between the first and second gradient pulses. The diffusion experiments were performed at constant δ and Δ values, using a series of 10 G values. To obtain absolute values for the self-diffusion coefficients, the field gradient strength was calibrated from measurements on reference 10% H_2O in D_2O and a 229 mM SDS sample (Jonstromer, Jonsson, & Lindman, 1991; Stilbs, 1982). The latter has a reported diffusion coefficient of 4×10^{-7} cm^2/s and an aggregation number of 64. The spectra were evaluated off-line utilizing nonlinear least squares fitting of the peak heights as a function of the gradient parameter, G^2, using Kaleida Graph (Reading, PA, USA) on a personal computer. The measured diffusion coefficient of the SDS micelle used in these studies was 1.8×10^{-7} cm^2/s, which would correspond to an estimated aggregation number of 83.

The release of DPH was determined by dispersing the LPs into 0.01% SDS solution in isotonic 20 mM sodium phosphate buffer adjusted to pH 7.4 and sonicating in a bath sonicator for 5 min. Aliquots of the LP dispersion were placed into a 96-well plate along with 10% SDS and/or 0.01% SDS solutions to produce a range of concentrations of LP (61–2,290 μg/mL) and SDS (8.58–174 mM). Samples were prepared at room temperature, and the 96-well plate was loaded onto the spectrofluorimeter, which was also initially at room temperature. The fluorescent intensity was determined at 32, 37, or 42°C using an excitation wavelength of 360 nm and an emission wavelength of 530 nm. Unless otherwise noted, a kinetic program was used, and time zero was taken as the first measurement made after the system reached a temperature of 42°C. The time to warm the plate within the spectrofluorimeter was about 10 min. Each set of concentrations was prepared in triplicate, and the intensity was measured as a function of time.

The intensity was converted to concentration by preparing standard curves of known DPH concentrations in 10% SDS and in lauryl alcohol. Lauryl alcohol was chosen over MA because it is liquid at room temperature, which greatly simplified preparation of standards. For lauryl alcohol, the intensity was a linear function of DPH concentration from 0 to 3 μg/mL with a slope of 3,970 μg/mL. Because it is also a long chain saturated alcohol with two less methylenes than MA, the slope of the standard curve is expected to be very close but slightly smaller given that the fluorescence of DPH increases with a reduction in polarity of the solvent. In 10% SDS, the intensity as a function of concentration was fit to a second-order polynomial for the concentration range of 0–8 μg/mL with a linear term of 1,796 μg/mL. Varying the concentration of SDS above the critical micelle concentration (CMC) did not appreciably affect the intensity of DPH.

The concentration of DPH in 10 mM SDS was measured with time following the addition of DPH crystals and also after adding DPH within MA particles. Samples were equilibrated at room temperature for 72 h, and the fluorescent intensity was determined every 24 h at room temperature using an excitation wavelength of 360 nm and an emission wavelength of 530 nm. The intensity was converted to DPH concentration using standards of DPH in SDS. The solubility of DPH in MA was also

determined following incubation of 2 mg DPH in 1 mL MA at 42°C for 24 h. The fluorescent intensity was determined at 42°C and converted to DPH concentration using standards of DPH in lauryl alcohol.

RESULTS AND DISCUSSION

The particles prepared by ultrasonic atomization followed by reflux drying appeared spherical in shape as evident in scanning electron micrographs (data not shown). The melting point was near 38°C, which is slightly lower than that observed with the bulk material. In addition, the enthalpy was also somewhat smaller. The particles were readily dispersed in 0.01% SDS solutions at a concentration below the CMC of SDS. With dynamic light scattering, the volume-weighted mean particle size was found to be 910 nm with a narrow standard deviation of 81 nm. The DPH load in the particles was near 1.5% (wt/wt), which is greater than the solubility of DPH in lauryl alcohol. Thus for the LPs, DPH is likely to exist as a dispersed solid with a uniform, spherical matrix of MA at room temperature. With an increase in temperature to 42°C, MA will melt, and the LPs will be transformed into particles composed of liquid MA.

In Figure 1, the results from the initial study exploring the relationship between fluorescent intensity and particle concentration, temperature, and SDS concentration are given. Here, the observed fluorescent intensity is plotted as a function of time for four different concentrations of particles (0.57–2.29 mg/mL). Beginning with the far left side of the figure, the observed intensity at 25°C depended on particle concentration but remained relatively constant with time. With an increase in temperature, the intensity increased and then remained constant. A similar change, albeit larger in magnitude, was observed when the temperature was increased to 42°C. The increase in intensity may arise partly from a change in the refractive index of the particles with melting, changes in the absorptivity and/or quantum yield of DPH, and/or the amount of DPH dissolved in the particles increased. Changes in the slope and intercept of the standard curves with temperature were small, which suggests that the intensity changes with temperature were likely to be a result of an increase in the solubility of DPH with temperature. If the intensity changed from an increase in solubility as would be expected from melting the particles, then the dissolution rate was very rapid, as the intensity underwent an apparent instantaneous change with temperature, followed by no further change in the next 20 min of observation.

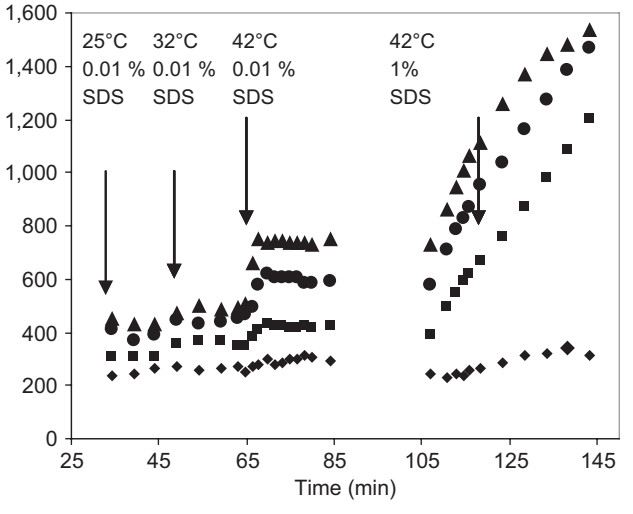

FIGURE 1. Intensity of DPH measured as a function of time during which the temperature and SDS concentration was varied as indicated on the figure at particle concentrations of (◆) 0.57, (■) 1.14, (●) 1.71, and (▲) 2.29 mg/mL.

In the far right-hand side of the figure, the effect of adding an aliquot of 10% SDS, while maintaining the temperature at 42°C, is shown. This addition resulted in a well concentration of 1% SDS. With the elevated temperature and higher SDS concentration, the intensity increased with time and the rate of increase was larger for the higher particle concentrations. An additional study revealed that incubating the particles in 1% SDS at a temperature of 37°C resulted in no change in intensity with time over a 20-min evaluation period. These results suggest that achieving a continual and measurable change in fluorescent intensity with time requires that the LPs be present with SDS micelles and at a temperature above the melting point of MA.

The fluorescent intensity of the same concentration of DPH is greater in lauryl alcohol than in a SDS solution, as can be inferred from the slopes of the standard curves given in the materials and methods section. Thus, simple transfer of DPH from the donor LPs to the acceptor SDS micelles should result in a decrease in the observed intensity, because the DPH moves from an environment of higher absorptivity/fluorescent quantum yield to one of lower values (Bondarev & Bachilo, 1990). However, as the intensity increases with time, DPH is likely present in the LP as a suspension and the transfer of DPH from the LP to the SDS micelle is accompanied by additional DPH dissolving within the LP. If true, then the total concentration of DPH within the particles decreases with time, but the DPH concentration in solution in the particle remains essentially constant. This is also consistent with the above conjecture that the change in intensity with a change in temperature was a result from an increase in the solubility coupled with virtually instantaneous dissolution. Thus, the increase in intensity with time is a result of DPH accumulation within the SDS micelles. Moreover, the mass of DPH accumulated with time within the micelle may be calculated from the slope of the intensity as a function of time and the standard curve.

In Figure 2, representative release curves are shown from the design study that was conducted in which the particle and SDS concentration were varied. In Figure 2, the concentration of DPH is given as a function of time for a particle concentration of 183 μg/mL and at SDS concentrations of 8.58, 17.2, 34.3, 68.7, and 103 mM. Each data point represents a mean of

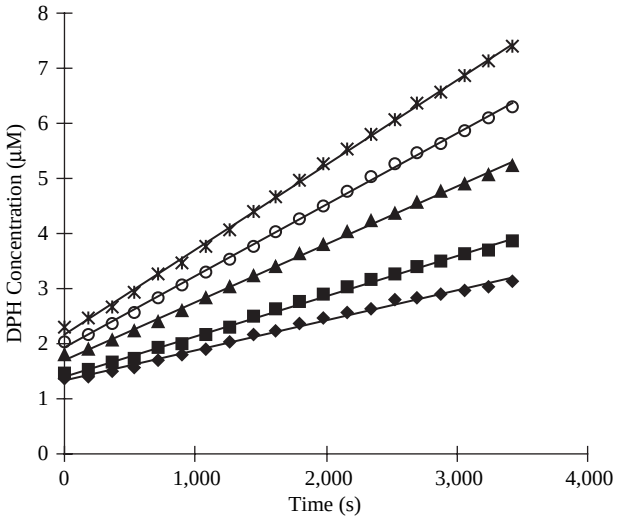

FIGURE 2. Concentration of DPH given as a function of SDS concentration of (◆) 8.58, (■) 17.2, (▲) 34.3, (○) 68.7, and (*) 103 mM. The solid lines represent best fits using a linear function. Particle concentration was 183 μg/mL.

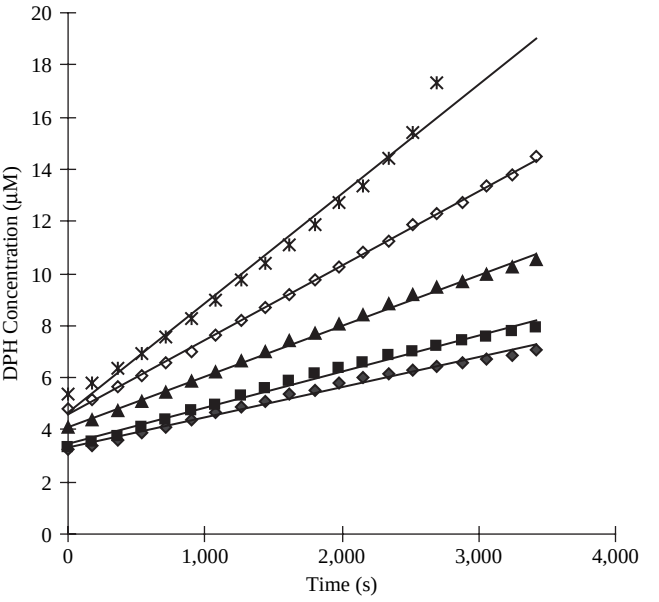

FIGURE 3. Concentration of DPH given as a function of SDS concentration of (◆) 8.58, (■) 17.2, (▲) 34.3, (◇) 68.7, and (*) 103 mM. The solid lines represent best fits using a linear function. Particle concentration was 428 μg/mL.

three observations, and the error bars have been omitted for clarity because the standard deviation was quite small (<5%). The solid lines/curves represent the results from regression of the data using a linear fit. For the three profiles in Figure 2, which are at the higher SDS concentrations, the DPH concentration increased linearly with time. This indicates that most of the above nonlinearity observed in Figure 1 arises from the nonlinear standard curve of DPH in SDS micelles. It can also be seen that the rate of increase as measured by the slope of the lines was larger for those wells that contained a higher concentration of SDS.

For the data that was obtained at the two lower SDS concentrations (Figure 2), the profiles are slightly nonlinear with negative curvature. Under the buffer and salt conditions, the estimated CMC of SDS is 1.6 mM, and thus the concentration of SDS in micelles at a total concentration of 8.58 mM is only 7 mM. The solubility of DPH in 10 mM SDS at 25°C was determined to be 3.10 μM, which indicates that there was a loss of sink conditions during the release study. That is, the DPH concentration in the micellar solution is no longer less than 15% of the saturation value, and therefore the release rate declines as the concentration of DPH in the micellar solution rises.

In Figure 3, which was obtained at the same SDS concentrations but at a higher particle concentration of 428 μg/mL, the two middle profiles are seen to be linear. The lower two curves are nonlinear with negative curvature as described above. It can be noted that the curvature is greater at this higher particle concentration, consistent with the explanation of nonsink conditions. In contrast, the uppermost curve, which contained the highest particle concentration and highest SDS concentration, is nonlinear with positive curvature. This may be a result of a loss of particle integrity that introduced an additional mechanism of release. The phase diagram has been reported for a number of compositions of SDS/MA/water, and the composition in the well falls within the two-phase regime, which indicates that the particles eventually will be disrupted, but are kinetically trapped for most of the experimental time frame (Epstein & Ross, 1957; Ma, Friberg, & Neogi, 1989). Nevertheless, separate studies involving SEM and dynamic light scattering failed to demonstrate a change in size, but this may reflect the insensitivity of these techniques to detect the small change that is needed to produce the nonlinearity.

For each release profile, linear regression was performed, and the resulting slope and associated 95% confidence limit were obtained. For the evidently nonlinear release profiles, a second-order polynomial was used to fit the data, and the coefficient of the linear term was identified. The slopes or linear terms were converted to molecules released per unit time and then plotted as a function of particle number concentration, which was calculated using the volume-weighted mean diameter (910 nm), the density of MA (0.8622 g/mL), and the known particle mass concentration in the well. In Figure 3, the plots are given where each set of data represents a different SDS concentration. Each set was then fit with a linear function where the intercept was forced through the origin. As can be seen, reasonably good fits were obtained with the correlation coefficients ranging from 0.925 to 0.997, and the higher concentrations of SDS were associated with larger slopes.

The effect of SDS concentration on the release rate was assessed as follows. The release rate was first divided by the

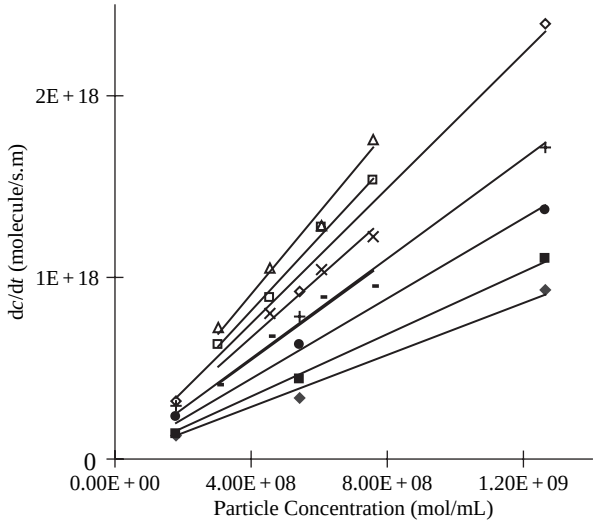

FIGURE 4. Release rate of DPH in molecules/second plotted as a function of particle concentration at different SDS concentrations. The solid lines represent the best fits using linear regression.

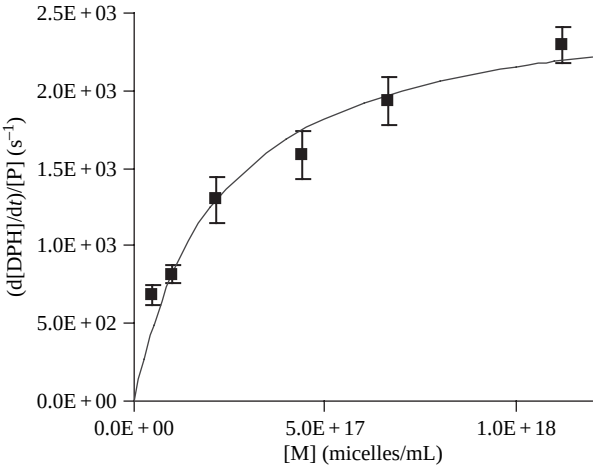

FIGURE 5. Normalized release rate of DPH in molecules/particle/second plotted as a function of micelle concentration. The solid line represents the best fit to a rectangular hyperbolic function.

particle number concentration. With the release rate thus normalized to particle number, it was then plotted as a function of micelle number (Figure 5), which was calculated using a CMC of 1.6 mM, an aggregation number of 83, and the known total concentration of SDS (Evans & Wennerström, 1999). In contrast to the linear effect of particle concentration, the rate of released increased with micelle concentration but in an evidently nonlinear manner. As shown previously in Figure 1, the release rate without the addition of micelles was zero, so the line must pass through the origin. At the other extreme of high micelle concentration, there is an indication that the rate is approaching a plateau. The data were fit using nonlinear regression to a rectangular hyperbolic function yielding two parameters: the maximum velocity of release, V_m, and the micelle concentration, K_m, producing a velocity equal to one half of V_m. (Chan et al., 1976; Prudich & Henry, 1978). The values obtained were 2,630 DPH molecules released per particle per second for V_m and 2.21 × 1,017 micelles/mL for K_m .

The nonlinear increase in release rate per particle with increasing micelle concentration provides a means to identify a mechanism consistent with the release profile. Because these values are the initial, linear release rates from the particles, the nonlinearity cannot be ascribed to a nonlinear increase in the solubility of DPH with increasing micelle concentration. The contribution arising from diffusional resistance within the particle can be assessed as follows. During release, the particles, which are composed of primarily MA, are in the liquid state. To evaluate the state of DPH in these liquid particles, the solubility of DPH in a SDS solution was measured with the addition of DPH crystals and with the addition of MA particles containing DPH. The solubilities of DPH were found to be 3.10 ± 0.21 and 38.7 ± 3.6 μM, respectively. Because the observed concentration of DPH presented in particles is greater than 10 times that when DPH is presented as a crystal, DPH in the particles is not at equilibrium but in a higher energetic state. As such, the MA particles contain a supersaturated solution of DPH, which can readily mix within the LPs. The instantaneous change in intensity with temperature also suggests that dissolution of DPH within the particle is not rate limiting.

The final consideration for the resistance to release of DPH is the possibility of depletion of the concentration within the particles. However, there are an estimated 10^7 molecules of DPH contained within each particle and even at the greatest extent of release, less than 0.1% was released. Thus, during the release study, DPH is maintained as a supersaturated solution within the liquid MA particles, and the contribution to the overall resistance to release is negligible.

Release of hydrophobic compounds from particles can also depend on the solute diffusion through the boundary layer, especially when it is solubilized by micelles. However, this too can be shown to be an unlikely contribution to the resistance, if the concentration of particles and micelles are considered. That is, the particle concentration was varied from just below 2×10^8 to over 10^9 particles/mL. As such, the near 1-μm particles are separated on average by an average distance of 10–20 μm, which is the typical magnitude of the diffusional boundary layer thickness. In addition, the micelle concentration ranged from 4.6 to 112 × 10^{16} micelles/mL. Here, the separation between micelles, which have an estimated diameter of 4.4 nm, is between 10 and 30 nm. Finally, at the maximum concentration of DPH in solution, only 1 in 11 micelles contained a DPH molecule, and more typically it was 1 in 100. These features are shown schematically in Figure 6, which is approximately drawn to scale.

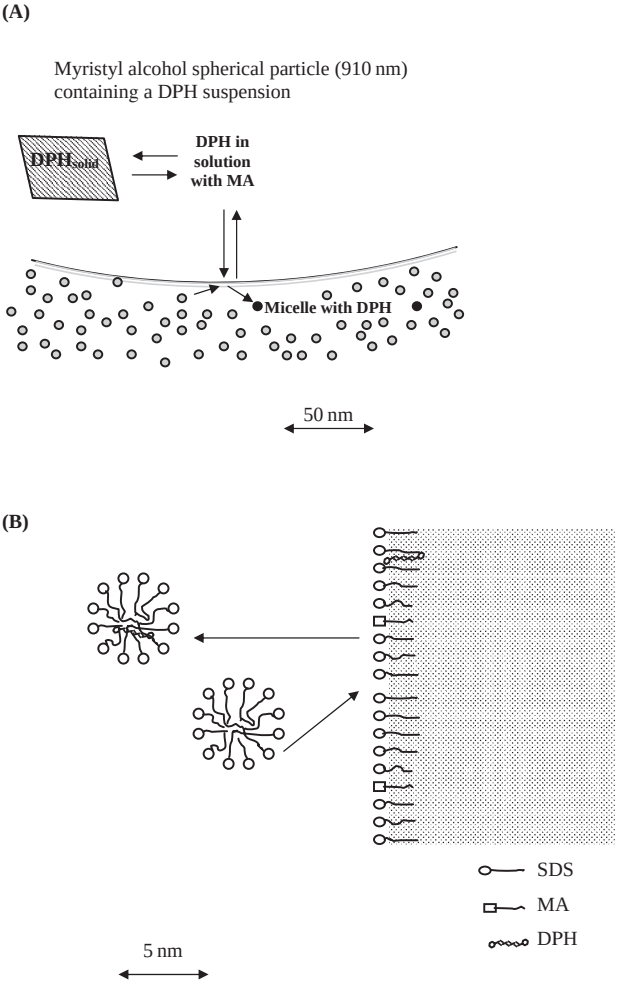

FIGURE 6. (A) Schematic representation of the release of DPH depicting the solid DPH dispersed in the liquid myristyl alcohol particle with surrounding SDS micelles. The solid circles represent micelles containing DPH. (B) Expanded view depicting individual micelles near particle surface.

In light of these considerations, a more reasonable conceptualization of the release involves SDS micelles colliding with the surface of the particle, during which time the micelle may or may not remove a DPH molecule from the particle (Chan et al., 1976). Collision theory has its roots in the kinetic theory of gases (Moore, Pearson, & Frost, 1981), and the approach used here is based on the Smoluchowski equation, which considers the number of times the micelles will undergo collisions with the particles in unit time and volume. Based on noninteracting hardcore spheres, the expression is as follows:

$$\frac{dN}{dt} = 4\pi d_{PM} D N_P N_M,$$

where d_{PM} is the collision cross section, $d_{PM} = (d_P + d_M)/2 \approx (1/2)d_P$, D is the diffusion coefficient, $D = 0.5(D_P + D_M) \approx 0.5D_M$, and N_M and N_P are the number densities for the micelles and particles, respectively. If release depends on collisions, then the rate should be linearly dependent on particle and micelle concentration.

In this study, the number of collisions the micelles will make with one particle will depend on the micelle concentration and ranged from 5.44 to 132×10^7 s^{-1}. This assumes the particles are composed of noninteracting, hardcore spheres. Because the maximum release rate was about 2,630 DPH molecules/s, the vast majority of collisions were ineffective in causing the release of DPH. In contrast, the collision rate among micelles is on the order of 1,020 s^{-1}, which is a consequence of the high concentration of micelles. Given this high rate of collisions among the micelles, it suggests that the number of collisions that the micelles make with the particles may be overestimated. In addition, the particles are expected to have adsorbed SDS molecules at the surface, which may affect the approach of SDS micelles to the particle surface and/or the collision frequency.

SUMMARY

Due to the hydrophobic nature and associated limited water solubility, the release of DPH is dependent on the presence of micelles. In addition, the release appears to depend on micellar collisions of the particles. The requirement of heating the particles for release provides a means to control not only the timing but also the site of drug release. This principle may be of value for temporal and spatial selectivity of drug delivery.

ACKNOWLEDGMENTS

This work was supported in part by the Undergraduate Research Opportunities Program (to J. M.) at the University of Minnesota.

REFERENCES

Aoki, H., Kakinuma, K., Morita, K., Kato, M., Uzuka, T., Igor, G., Takahashi, H., Tanaka, R. (2004). Therapeutic efficacy of targeting chemotherapy using local hyperthermia and thermosensitive liposome: Evaluation of drug distribution in a rat glioma model. *Int J Hyperthermia, 20*(6), 595–605.

Bondarev, S. L., & Bachilo, S. M. (1990). Solvent and temperature effects on fluorescence and absorption from the S1 states in diphenylpolyenes. *J. Appl. Spectrosc., 53*(5), 1142–1147.

Chan, A. F., Evan, D. F., & Cussler, E. L. (1976). Explaining solubilization kinetics. *AIChE J., 22*(6), 1006–1012.

Epstein, M. B., & Ross, J. (1957). Solubility of lauryl alcohol in aqueous solutions of sodium lauryl sulfate. *J. Phys. Chem., 61*, 1578.

Evans, D. F., & Wennerström, H. (1999). *The colloidal domain: Where physics, chemistry, biology, and technology meet*. New York: Wiley-VCH.

Hitzman, C. J., Elmquist, W. F., Wattenberg, L. W., & Wiedmann, T. S. (2006). Development of a respirable, sustained release microcarrier for 5-fluorouracil I: In vitro assessment of liposomes, microspheres, and lipid coated nanoparticles. *J Pharm Sci., 95*(5), 1114–1126.

Jonstromer, M., Jonsson, M., & Lindman, B. (1991). Self-diffusion in nonionic surfactant-water systems. *J. Phys. Chem., 95*(8), 3293–3300.

Lao, L. L., & Ramanujan, R. V. (2004). Magnetic and hydrogel composite materials for hyperthermia applications. *J. Mater. Sci. Mater. Med., 15*(10), 1061–1064.

Ma, Z. N., Friberg, S. E., & Neogi, P. (1989). Single-component mass transfer in a cosurfactant-water-surfactant system. *AIChE J.*, *35*(10), 1678–1684.

Mehnert, W., & Mader, K. (2001). Solid lipid nanoparticles production, characterization and applications. *Adv. Drug Deliv. Rev.*, *47*, 165–169.

Moore, J. W., Pearson, R. G., & Frost, A. A. (1981). *Kinetics and mechanism*. New York: Wiley.

Needham, D., Anyarambhatla, G., Kong, G., & Dewhirst, M. W. (2000). A new temperature-sensitive liposome for use with mild hyperthermia: Characterization and testing in a human tumor xenograft model. *Cancer Res.*, *60*(5), 1197–1201.

Prudich, M. E., & Henry, J. D. (1978). The mechanisms of transfer of hydrophobic coated mineral matter particles from a hydrocarbon to an aqueous phase. *AIChE J.*, *24*(5), 788–795.

Stilbs, P. (1982). Fourier transform NMR pulsed-gradient spin-echo (FT-PGSE) self-diffusion measurements of solubilization equilibria in SDS solutions. *J. Colloid Interface Sci.*, *87*(2), 385–394.

Venkateswarlu, V., & Manjunath, K. (2004). Preparation, characterization and in vitro release kinetics of clozapine solid lipid nanoparticles. *J. Control. Release*, *95*(3), 627–638.

Wiedmann, T. S., & Hitzman, C. J. (2004). Reflux drying of aerosols. *J Aerosol Med.*, *17*(4), 344–353.

Wissing, S. A., Kayser, O., & Muller, R. H. (2004). Solid lipid nanoparticles for parenteral drug delivery. *Adv. Drug Deliv. Rev.*, *56*(9), 1257–1272.

Wong, H. L., Bendayan, R., Rauth, A. M., Li, Y. Q., & Wu, X. Y. (2007). Chemotherapy with anticancer drugs encapsulated in solid lipid nanoparticles. *Adv. Drug Deliv. Rev.*, *59*, 491–504.

Xiang, Q. Y., Wang, M. T., Chen, F., Gong, T., Jian, Y. L., Zhang, Z. R., Huang, Y. (2007). Lung-targeting delivery of dexamethasone acetate loaded solid lipid nanoparticles. *Arch. Pharm. Res.*, *30*(4), 519–525.

Zara, G. P., Bargoni, A., Cavalli, R., Fundaro, A., Vighetto, D., & Gasco, M. R. (2002). Pharmacokinetics and tissue distribution of idarubicin-loaded solid lipid nanoparticles after duodenal administration to rats. *J. Pharm. Sci.*, *91*(5), 1324–1333.

Zara, G. P., Cavalli, R., Bargoni, A., Fundaro, A., Vighetto, D., & Gasco, M. R. (2002). Intravenous administration to rabbits of non-stealth and stealth doxorubicin-loaded solid lipid nanoparticles at increasing concentrations of stealth agent: pharmacokinetics and distribution of doxorubicin in brain and other tissues. *J. Drug Target*, *10*(4), 327–335.

zur Muhlen, A., Schwarz, C., & Mehnert, W. (1998). Solid lipid nanoparticles (SLN) for controlled drug delivery—drug release and release mechanism. *Eur. J. Pharm. Biopharm.*, *45*(2), 149–155.

Copyright of Drug Development & Industrial Pharmacy is the property of Taylor & Francis Ltd and its content may not be copied or emailed to multiple sites or posted to a listserv without the copyright holder's express written permission. However, users may print, download, or email articles for individual use.